Adaptive Central-upwind Weighted Compact Non-linear Scheme with Increasing Order of Accuracy

†Kamyar Mansour[1], Kaveh Fardipour[1]

[1]Department of Aerospace Engineering, Amirkabir University of Technology, 424 Hafez Ave, Tehran, Iran.

†Corresponding author: mansour@aut.ac.ir

Abstract

In this work, effect of using an adaptive central-upwind (ACU) interpolation on weighted compact non-linear scheme (WCNS) is investigated. Based on the smoothness of solution, this type of interpolation adapts between central and upwind stencils by a weighting relation and combination of smoothness indicators of the optimal high-order stencil and its sub-stencils. The coefficients of sixth to tenth order ACU-WCNS are calculated. To evaluate basic numerical characteristics of this new schemes truncation error analysis and wavenumber analysis is performed and by applying ACU-WCNS on several benchmark problems, its shock-capturing abilities, its behavior in presence of severe discontinuity and its numerical resolution in shock-entropy interaction are investigated.

Keywords: High-order numerical method; Weighted compact nonlinear scheme; Shock-capturing; Compressible flow.

Introduction

Over past three decades there were many efforts for development of high-order numerical methods that simultaneously have the capability to capture flow discontinuity and resolve small-scale features of flow. Weighted Essentially Non-oscillatory (WENO) [1] scheme and Weighted Compact Nonlinear Scheme (WCNS) [2] scheme are two families of such numerical methods.

The WENO scheme is based on Essentially Non-oscillatory (ENO) scheme [3], but instead of using only one of sub-stencils, it uses a weighted combination of all sub-stencils. This scheme was developed in finite volume framework by Liu et al. [4]. Jiang and Shu [1] extended the WENO scheme to finite difference framework and proposed a new formulation for nonlinear weights to increase order of accuracy and later Balsara and Shu [5] and Gerolymos et al. [6] studied the high order behavior of the WENO scheme.

Despite having high order of accuracy and good shock capturing capabilities, the WENO scheme also has some shortcomings. One of the problems with the original WENO scheme of Jiang and Shu [1] is loss of accuracy near critical points. Analysis of Henrick et al. [7] showed this loss of accuracy is because of nonlinear weights and they purposed a mapping method for computation of nonlinear weights to prevent loss of accuracy. Borges et al. [8] also purposed a new method for computation of nonlinear weights of fifth order WENO to avoid loss of accuracy and later expanded it for higher order of accuracy [9], their method has lower computational cost in comparison to Henrick et al. [7] mapping method.

There are several ways to reduce numerical dissipation of the WENO scheme. One them is hybrid methods which only use the WENO scheme in vicinity of discontinuities and use another scheme with lower or no numerical dissipation in smooth regions [10]-[12]. Another way is to optimize dissipation and dispersion error [13]-[15], this usually achieved by finding optimal coefficients or linear weights by minimizing integral error following optimizing procedures of Tam and Webb [16] and Zhuang and Chen [17]. A more recent way for reduction of numerical dissipation of the WENO scheme is adaptive central-upwind WENO (ACU-WENO) scheme [18]-[20]. Based on smoothness of solution, this new family of WENO scheme can adapt between central and upwind stencils and achieves higher order of accuracy, numerical resolution and lower dissipation by using a central stencil in smooth regions of solution.

The WCNS was originally developed by Deng and Zhang [21] and later extended to higher order of accuracy by Nonomura et al. [22] and Zhang et al. [23]. This scheme is a combination of compact scheme [24] and WENO interpolation [25]. This scheme includes a node-to-midpoint weighted interpolation and a midpoint-to-node differencing and has three advantages over finite difference WENO scheme [26]:

1- Slightly higher numerical resolution;
2- Compatibility with different flux treatments;
3- Better performance on general curvilinear grids [27].

Nonomura and Fujii [28] studied effects of different types of midpoint-to-node differencing methods on WCNS and they showed it does not significantly change numerical resolution and shock capturing capabilities of WCNS. Nonomura and Fujii [26] proposed a new formulation for midpoint-to-node differencing, which significantly increases robustness of WNCS. Recently Sumi and Kurotaki [29] used a sixth order adaptive central-upwind interpolation with robust formulation of a tridiagonal midpoint-to-node differencing to improve numerical resolution and robustness of original WCNS [21]. Some studies [22][30]-[32] showed increasing the order of accuracy of numerical method, will increase computational efficiency. Therefore in this paper we intend to study ACU-WCNS with order of accuracy higher than sixth.

Construction of the Numerical Scheme

For numerical solution of a conservation law as

$$\frac{\partial u}{\partial t}+\frac{\partial f(u)}{\partial x}=0, \tag{1}$$

where t is time, x is a spatial dimension, u is function of x and t and f is flux function, Eq. (1) can be written in a semidiscretized form as

$$\left(\frac{\partial u}{\partial t}\right)_i=-f_i', \tag{2}$$

where f_i' is an approximation of spatial derivative of f on grid point x_i. Following Lele [24], for computation of f_i' in Eq. (2) we can use a linear formulation as

$$f_i'+\sum_{j=1}^{M}a_j\left(f_{i+j}'+f_{i-j}'\right)=\frac{1}{h}\sum_{k=1}^{N}b_l\left(f_{i+k-\frac{1}{2}}-f_{i-k+\frac{1}{2}}\right), \tag{3}$$

where M and N are positive integers. We can derive the coefficients a_j and b_l by matching the Taylor series coefficients [24]. The robust formulation of Nonomura and Fujii [26], which uses a midpoint-and-node-to-node differencing, can be written in a general form as

$$f_i'+\sum_{j=1}^{M}a_j\left(f_{i+j}'+f_{i-j}'\right)=\frac{1}{h}\sum_{k=1}^{N}c_k\left(f_{i+\frac{k}{2}}-f_{i-\frac{k}{2}}\right), \tag{4}$$

Following Nonomura and Fujii [28] we only use explicit form of Eq. (3) and Eq. (4) (i.e. $a_j=0$). For explicit form of these equations, the coefficients are listed in [28] and we list them again in Table 1 and Table 2, respectively for Eq. (3) and Eq. (4).

Table 1. Coefficients for Eq. (3) [28]

Coefficients	b_1	b_2	b_3	b_4	b_5
Fourth-order explicit	$\frac{9}{8}$	$-\frac{1}{24}$	0	0	0
Sixth-order explicit	$\frac{75}{64}$	$-\frac{25}{384}$	$\frac{3}{640}$	0	0
Eighth-order explicit	$\frac{1225}{1024}$	$-\frac{245}{3072}$	$\frac{49}{5120}$	$-\frac{5}{7168}$	0
Tenth-order explicit	$\frac{19845}{16384}$	$-\frac{735}{8192}$	$\frac{567}{40960}$	$-\frac{405}{229376}$	$\frac{35}{294912}$

Table 2. Coefficients for Eq. (4) [28]

Coefficients	c_1	c_2	c_3	c_4	c_5
Fourth-order explicit	$\frac{4}{3}$	$-\frac{1}{6}$	0	0	0
Sixth-order explicit	$\frac{3}{2}$	$-\frac{3}{10}$	$\frac{1}{30}$	0	0
Eighth-order explicit	$\frac{8}{5}$	$-\frac{2}{5}$	$\frac{8}{105}$	$-\frac{1}{140}$	0
Tenth-order explicit	$\frac{5}{3}$	$-\frac{10}{21}$	$\frac{2}{42}$	$-\frac{5}{252}$	$\frac{1}{630}$

To interpolate midpoint values from node values (to save space we only write formulation for left-biased interpolation, which is shown by superscript L and the right-biased interpolation could be derived by mirroring the left-biased interpolation around $x_{i+\frac{1}{2}}$), in a stencil $S^{(2r-1)} = \left(x_{i-r+1},...,x_{i+r-1}\right)$ with $\left(2r-1\right)$ points and r substencils as $S_k^{(2r-1)} = \left(x_{i+k-r+1},...,x_{i+k}\right)$, we can use a linear formulation as

$$\hat{f}^{L}_{i+\frac{1}{2}} = \sum_{k=-r+1}^{r+1} d_k f_{i+k}, \tag{5}$$

where d_k is constant coefficient. If we consider r substencils as $S_k^{(2r-1)} = \left(x_{i+k-r+1},...,x_{i+k}\right)$ in $S^{(2r-1)}$, we can use a linear formulation as

$$\hat{f}^{L}_{i+\frac{1}{2}} = \sum_{k=0}^{r-1} d_k^r \hat{f}^{r}_{k,i+\frac{1}{2}}, \tag{6}$$

where d_k^r is linear weight and $\hat{f}^r_{k,i+\frac{1}{2}}$ is the interpolated value for each substencil. We can write $\hat{f}^r_{k,i+\frac{1}{2}}$ as

$$\hat{f}^r_{k,i+\frac{1}{2}} = \sum_{l=0}^{r-1} a^r_{k,l} f_{i-k+j}, \tag{7}$$

where $a^r_{k,l}$ is constant coefficient. The linear relation in Eq. (6) cannot capture discontinuities accurately. To solve this problem we can combine the substencil values of Eq. (7) by a nonlinear formulation as

$$\hat{f}^L_{i+\frac{1}{2}} = \sum_{k=0}^{r-1} \omega_k^r \hat{f}^r_{k,i+\frac{1}{2}}, \tag{8}$$

where ω_k^r is nonlinear weight and is given by

$$\omega_k^r = \frac{\alpha_k^r}{\sum_{l=0}^{r-1} \alpha_l^r}, \tag{9}$$

$$\alpha_k^r = \frac{d_k^r}{\left(\varepsilon + IS_k^r\right)^p}, k = 0, ..., r-1, \tag{10}$$

where ε is small positive value to avoid division by zero, p is a positive integer and IS_k^r is smoothness indicator and is given by

$$IS_k^r = \sum_{l=1}^{r-1} \int_{x_{i-\frac{1}{2}}}^{x_{i+\frac{1}{2}}} \Delta x^{2l-1} \left(\frac{\partial^l f^{(r)}(x)}{\partial x^l} \right)^2 dx. \tag{11}$$

Hu et al. [19] proposed an alternative procedure for the WENO scheme which smoothly adapts between central and upwind stencils. According to this concept, to interpolate midpoint values from node values, instead of using biased stencil $S^{(2r-1)}$, we use a central stencil $S^{(2r)} = \left(x_{i-r+1}, ..., x_{i+r}\right)$ with $(2r)$ points and $r+1$ substencils. To include the new substencil, we should rewrite Eq. (5) to Eq. (8) as

$$\hat{f}^L_{i+\frac{1}{2}} = \sum_{k=-r+1}^{r} d_k f_{i+k}, \tag{12}$$

$$\hat{f}^L_{i+\frac{1}{2}} = \sum_{k=0}^{r} d_k^r \hat{f}^r_{k,i+\frac{1}{2}}, \tag{13}$$

$$\hat{f}^L_{i+\frac{1}{2}} = \sum_{k=0}^{r} \omega_k^r \hat{f}^r_{k,i+\frac{1}{2}}. \tag{14}$$

the nonlinear weight is given by

$$\omega_k^r = \frac{\alpha_k^r}{\sum_{l=0}^{r} \alpha_l^r}, \tag{15}$$

$$\alpha_k^r = d_k^r \left(C + \frac{\tau_{2r}}{\varepsilon + IS_k^r} \right), k = 0,...,r, \tag{16}$$

where C is a constant and $C \ll 1$. τ_{2r} is a new reference smoothness indicator. To avoid oscillations near discontinuities, instead of using IS_r^r in Eq. (16), we use IS_{2r} which is smoothness indicator of the complete stencil. To increase numerical resolution Hu and Adams [20] proposed a new formulation for computation of α_k^r

$$\alpha_k^r = d_k^r \left(C_q + \frac{\tau_{2r}}{IS_k^r + \varepsilon \Delta x^2} \frac{IS_{ave}^r + \chi \Delta x^2}{IS_k^r + \chi \Delta x^2} \right)^q, k = 0,...,r, \tag{17}$$

where C_q is a constant and $C_q \gg C$. $\chi = \dfrac{1}{\varepsilon}$ and IS_{ave}^r is an average of smoothness indicator of different substencils and there is a relation between τ_{2r}, IS_{2r} and IS_{ave}^r as

$$\tau_{2r} = IS_{2r} - IS_{ave}^r. \tag{18}$$

Some values and formulas for d_k^r, $\hat{f}^r_{k,i+\frac{1}{2}}$, IS_k^r, IS_{2r} and IS_{ave}^r are given in appendix A.

Truncation Error Analysis

Following Hu et al. [19], in this we perform a truncation error to find sufficient condition for ACU-WCNS to achieve the designed order of accuracy. We can write below relations between $f_{i+\frac{1}{2}}$ and interpolated values $\hat{f}_{i+\frac{1}{2}}$ from Eq. (13) and $\hat{f}^r_{k,i+\frac{1}{2}}$ from Eq. (7)

$$\hat{f}_{i+\frac{1}{2}} = f_{i+\frac{1}{2}} + O(\Delta x^{2r}), \tag{19}$$

$$\hat{f}^r_{k,i+\frac{1}{2}} = f_{i+\frac{1}{2}} + A_k^r \Delta x^r + O(\Delta x^{r+1}). \tag{20}$$

We can rewrite Eq. (14) as

$$\hat{f}_{i+\frac{1}{2}} = \sum_{k=0}^{r} d_k^r \hat{f}^r_{k,i+\frac{1}{2}} + \sum_{k=0}^{r} \left(\omega_k^r - d_k^r \right) \hat{f}^r_{k,i+\frac{1}{2}}, \tag{21}$$

Using the first linear term on the right-hand-side of Eq. (21) in Eq. (3) or Eq. (4) leads to derivative of $O(\Delta x^{2r})$. Therefore the sufficient condition for Eq. (3) or Eq. (4) to be of $O(\Delta x^{2r})$ is that the term on the right-hand-side of Eq. (21) is at least $O(\Delta x^{2r+1})$. Using Eq. (20) we can expand this term as

$$\sum_{k=0}^{r} \left(\omega_k^r - d_k^r \right) \hat{f}^r_{k,i+\frac{1}{2}} = f_{i+\frac{1}{2}} \sum_{k=0}^{r} \left(\omega_k^r - d_k^r \right) + A_k^r \Delta x^r \sum_{k=0}^{r} \left(\omega_k^r - d_k^r \right) + O(\Delta x^{r+1}) \sum_{k=0}^{r} \left(\omega_k^r - d_k^r \right). \tag{22}$$

The first term on the right-hand-side of Eq. (22) is zero because of normalization of the weights, therefore the sufficient condition for having a $O(\Delta x^{2r})$ derivative is

$$\omega_k^r - d_k^r = O(\Delta x^{r+1}). \tag{23}$$

Numerical Examples

In this section, we provide some numerical examples to show shock-capturing capabilities and numerical resolution of the proposed ACU-WCNS scheme. These problems are described by compressible Euler equations

$$\frac{\partial}{\partial t}\begin{bmatrix} \rho \\ \rho u \\ E \end{bmatrix} + \frac{\partial}{\partial x}\begin{bmatrix} \rho u \\ \rho u^2 + p \\ (E+p)u \end{bmatrix} = 0, \tag{24}$$

where ρ is density, p is pressure, u is x component of velocity vector, E is total energy and related to pressure as $e = \frac{p}{\gamma - 1} + \frac{1}{2}\rho u^2$ and $\gamma = 1.4$ is the ratio of specific heats. To reduce numerical oscillations we use local characteristic decomposition by Roe averaged variables and we use the Lax-Friedrichs method for flux vector splitting. For time integration we use a third order TVD Runge-Kutta method [33]. We used Eq. (4) for midpoint-and-node-to-node differencing and Eq. (17) for calculation of α_k^r, $C_q = 1000$ and $q = 2(r-1)$.

In a series of benchmark problems, results of ACU-WCNS with six, eight and ten point stencils are compared with ninth order WENO-Z [9]. The first problem is Sod shock tube [34] and initial condition is defined as

$$(\rho, u, p) = \begin{cases} (1, 0, 1) & \text{if} \quad 0 < x < 0.5, \\ (0.125, 0, 0.1) & \text{if} \quad 0.5 < x < 1. \end{cases}$$

The second problem is Lax shock tube [35] and initial condition is

$$(\rho, u, p) = \begin{cases} (0.445, 0.698, 0.3528) & \text{if} \quad 0 < x < 0.5, \\ (0.5, 0, 0.571) & \text{if} \quad 0.5 < x < 1. \end{cases}$$

The third problem is 123 shock tube [36] with initial condition as

$$(\rho, u, p) = \begin{cases} (1, -2, 0.4) & \text{if} \quad 0 < x < 0.5, \\ (1, 2, 0.4) & \text{if} \quad 0.5 < x < 1. \end{cases}$$

We choose the fourth problem from Nonomura and Fujii [26]. This shock tube has a very high pressure ratio and includes a severe shock. Initial condition is

$$(\rho, u, p) = \begin{cases} (1, 0, 10000) & \text{if} \quad 0 < x < 0.5, \\ (0.125, 0, 0.1) & \text{if} \quad 0.5 < x < 1. \end{cases}$$

The fifth problem is from Toro [37] and this problem also includes a severe shock. Initial condition is

$$(\rho, u, p) = \begin{cases} (1, -19.59745, 1000) & \text{if} \quad 0 < x < 0.5, \\ (1, -19.59745, 0.01) & \text{if} \quad 0.5 < x < 1. \end{cases}$$

The last problem is the Shu-Osher problem [38] and initial condition is

$$(\rho,u,p)=\begin{cases}(3.857,2.629,10.333) & if \quad 0<x<1,\\(1+0.2\sin(5x),0,1) & if \quad 1<x<10.\end{cases}$$

Fig. (1) and Fig. (2) respectively show density distribution for the Sod and the Lax problems. All ACU-WCNS show good capturing abilities and there are no visible numerical oscillations. It should be noted some adaptive central-upwind [18] or optimized [15] WENO schemes have numerical oscillations in these problem and therefore we could conclude Hu et al [19] adaption mechanism also works well in ACU-WCNS.

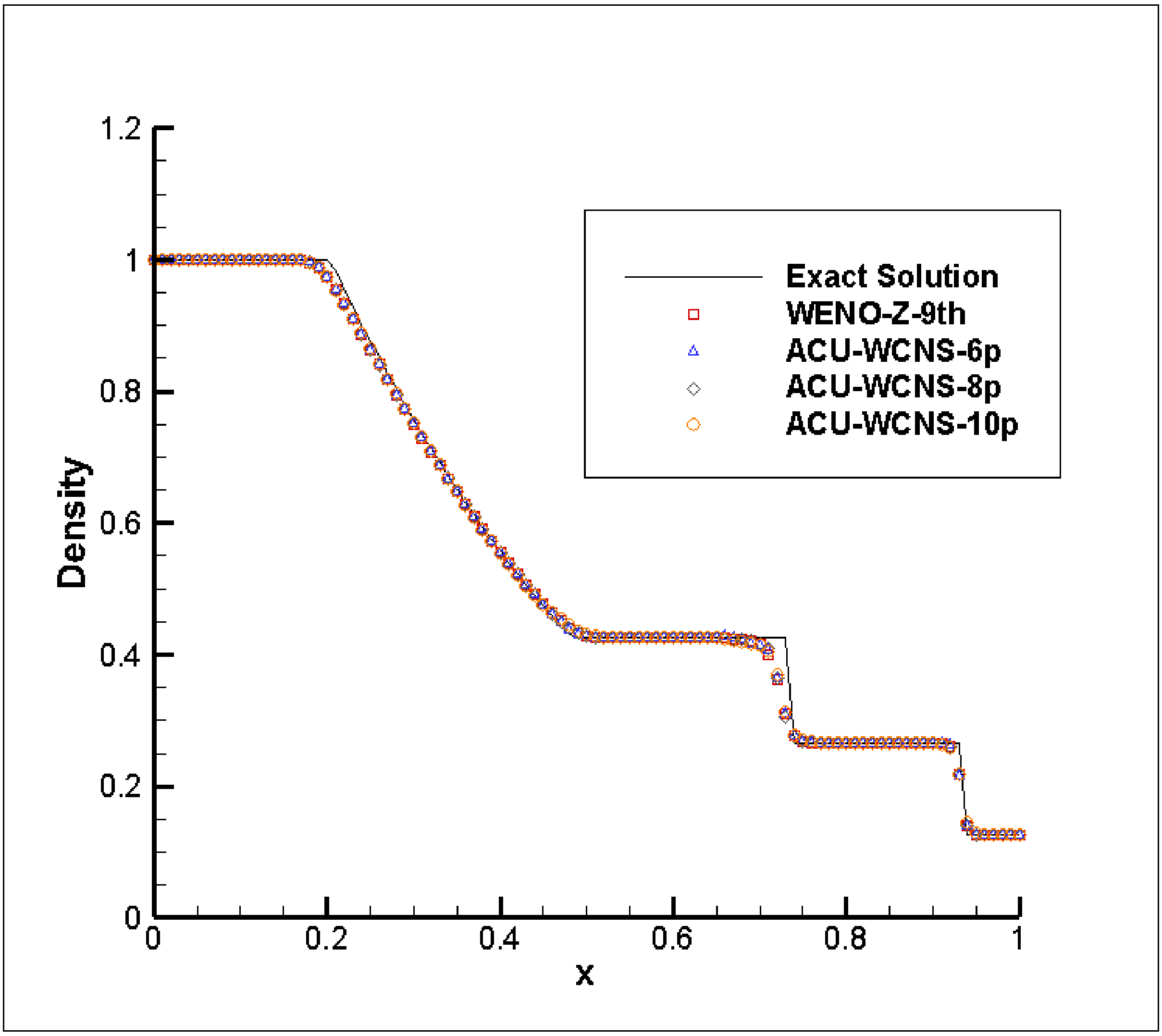

Figure 1. Density distribution for the Sod problem with 100 grid points at t=0.25 s

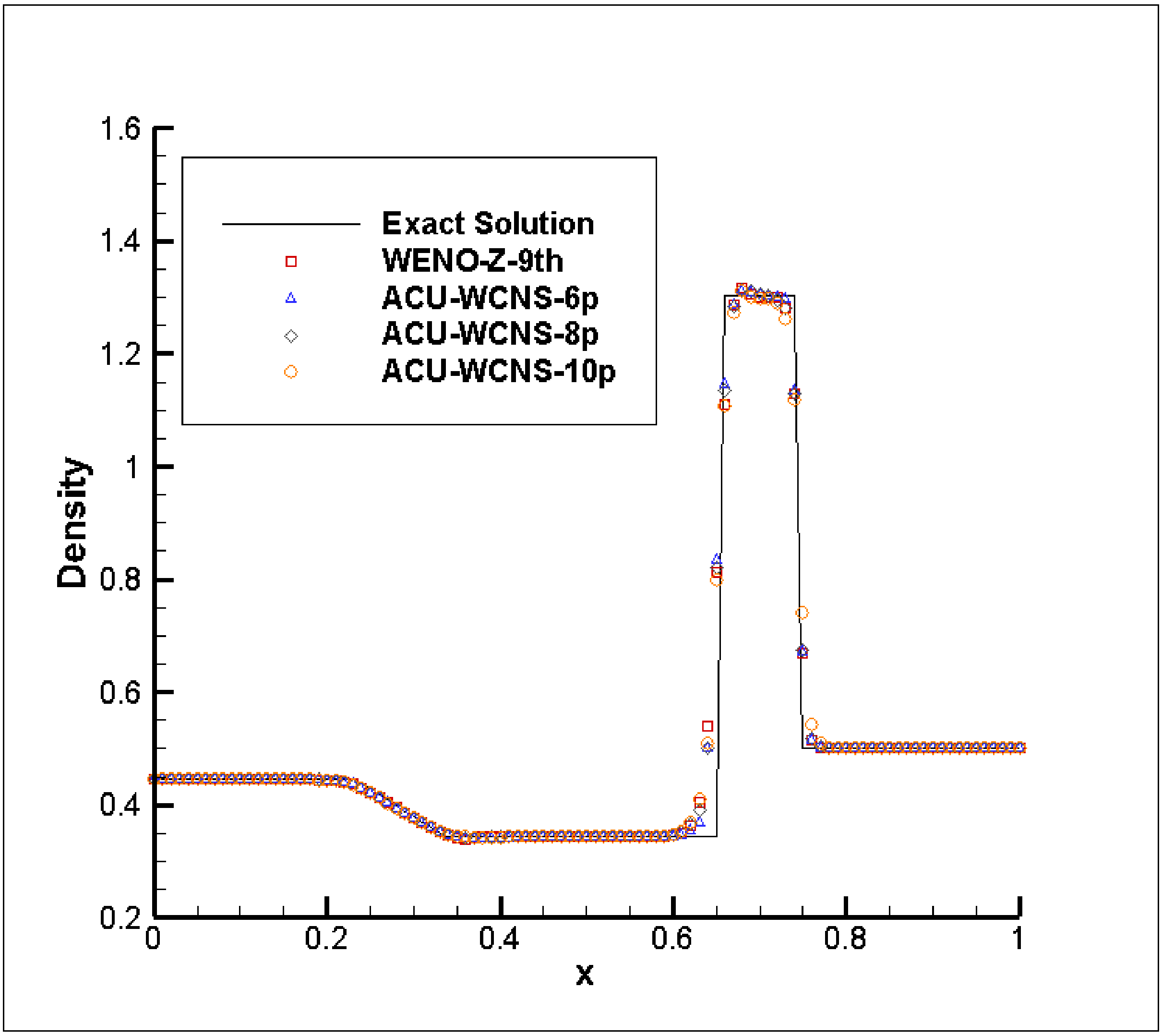

Figure 2. Density distribution for the Lax problem with 100 grid points at t=0.1 s

The third to fifth problems are cases with severe conditions and Fig. (3) to Fig. (5) show their density distribution. The 123 problem contains a near-vacuum condition and is suitable for assessment of numerical methods in low pressure and density situations. All ACU-WCNS show good results for this problem. The fourth and fifth problems contain strong shocks. All methods show good results except ACU-WCNS with ten points stencil, therefore this method is not as robust as other methods.

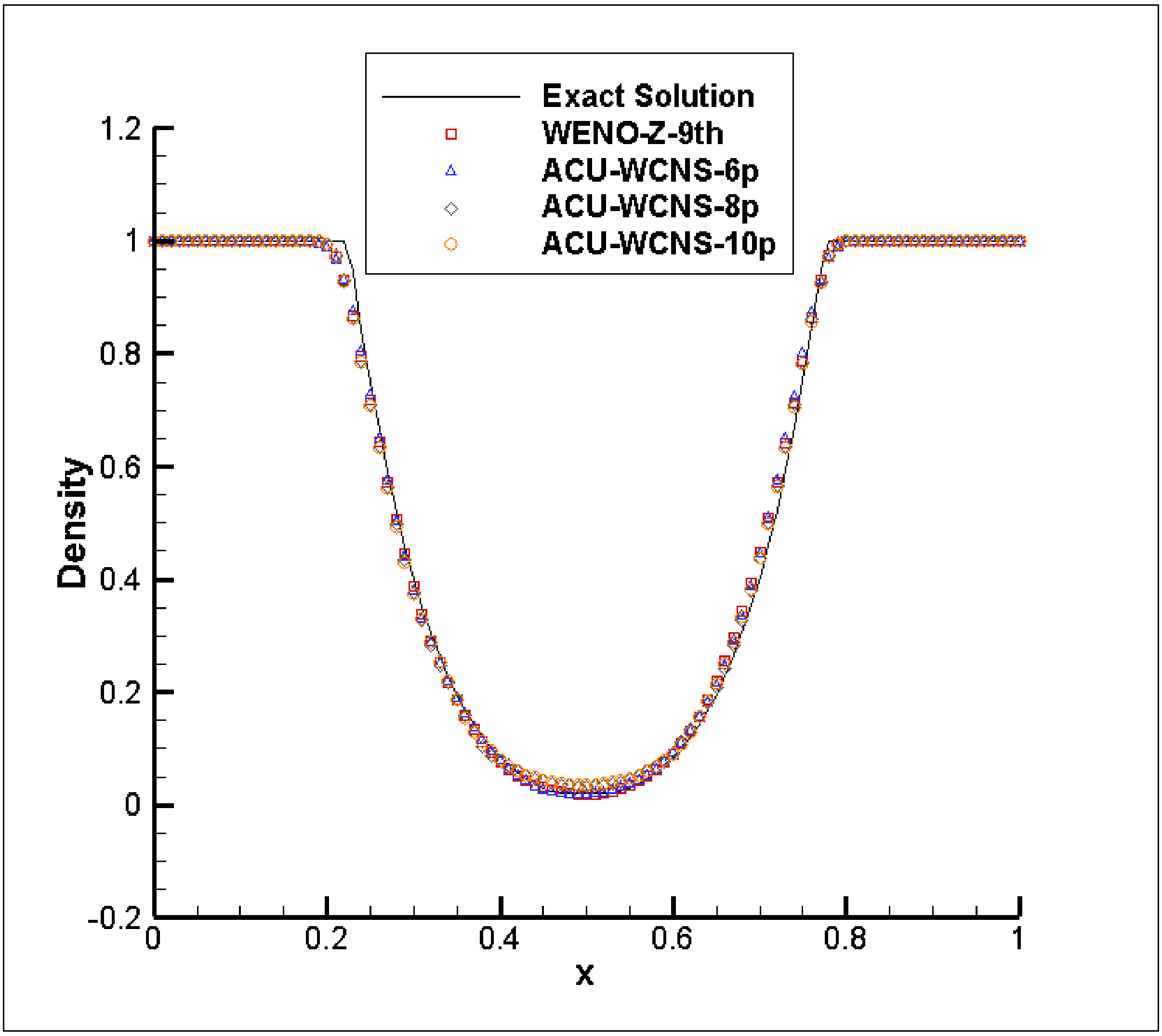

Figure 3. Density distribution for the 123 problem with 100 grid points at t=0.1 s

S

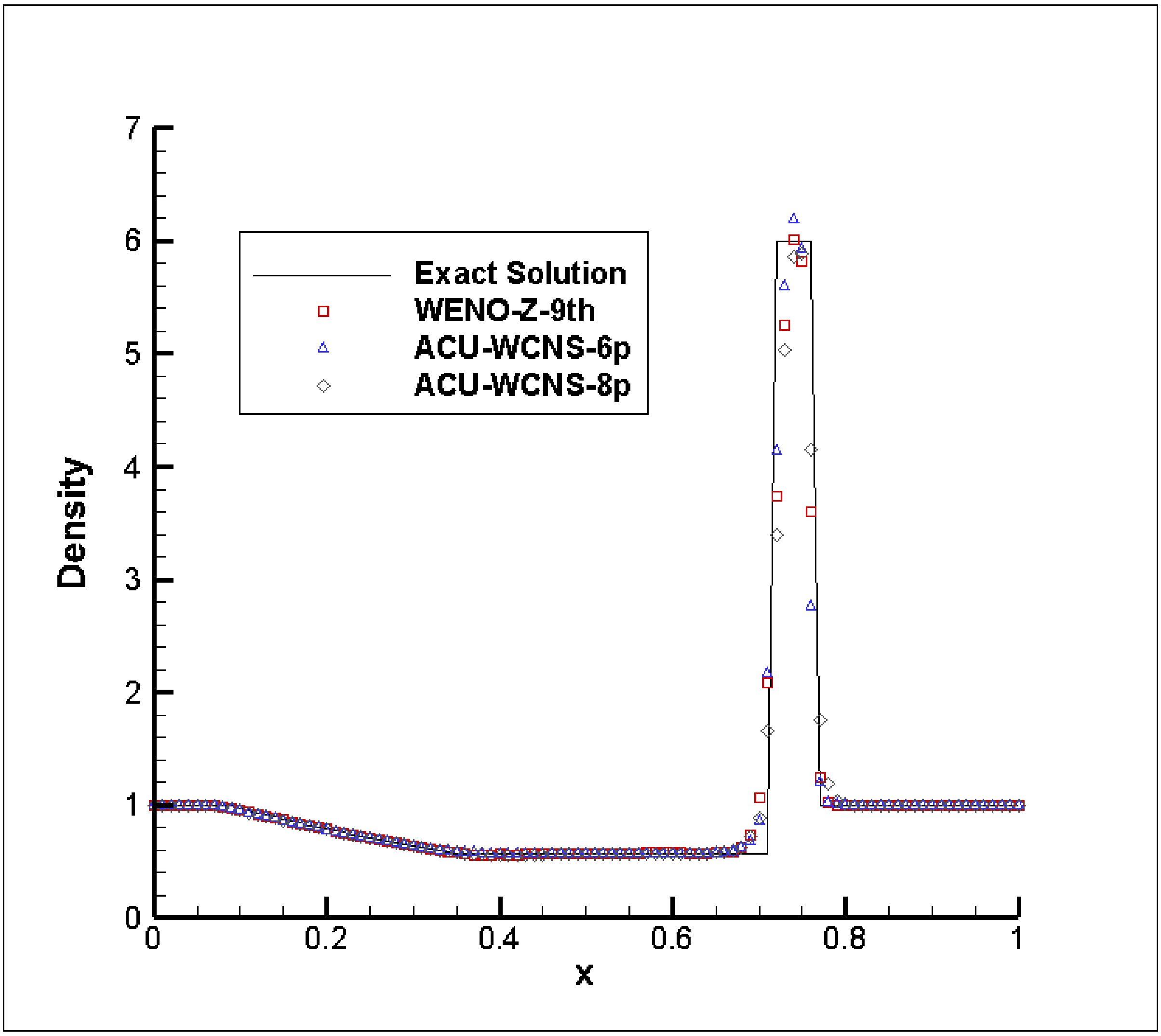

Figure 4. Density distribution for the forth problem with 100 grid points at t=0.0035 s

S

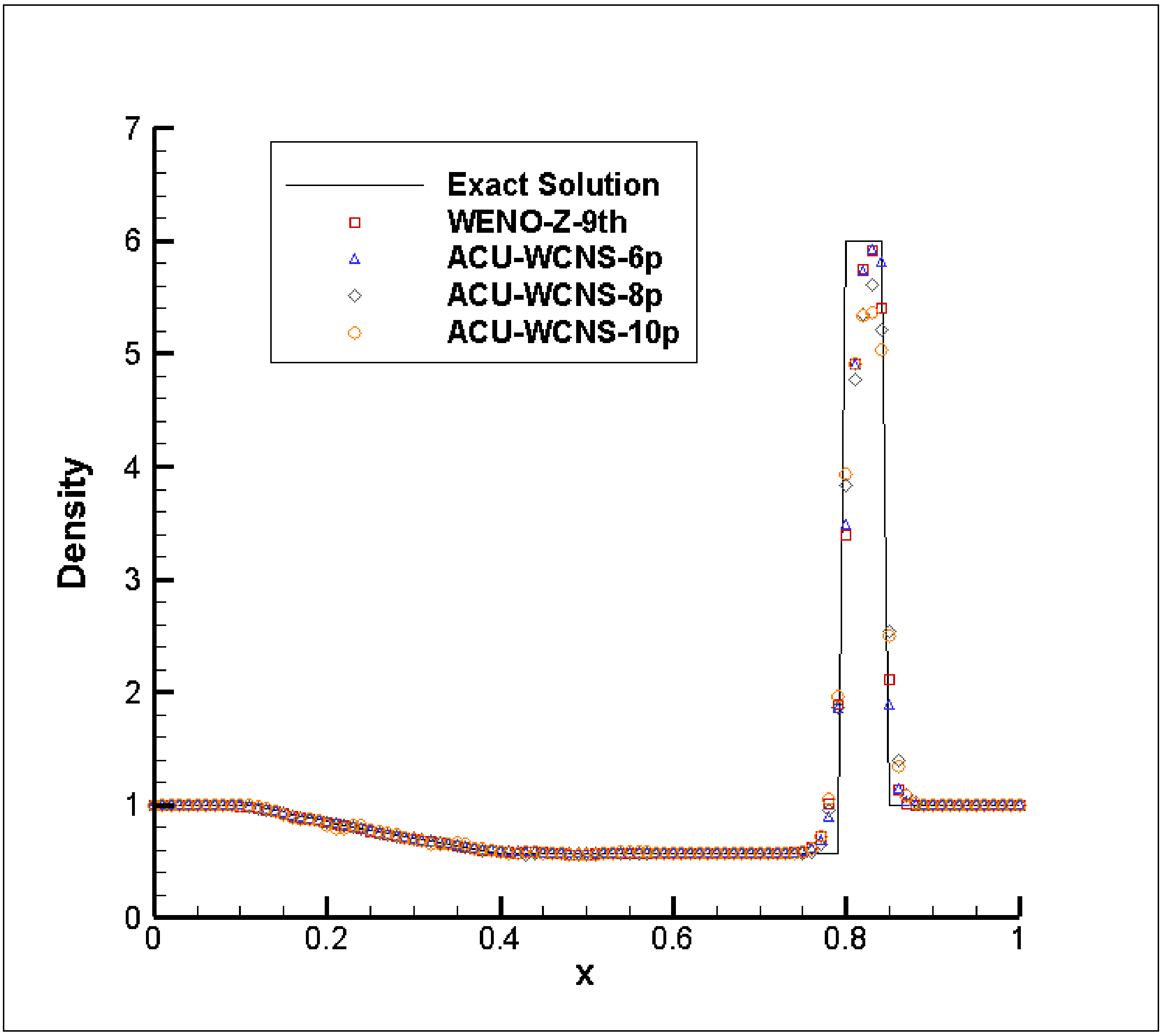

Figure 5. Density distribution for the fifth problem with 100 grid points at t=0.012 s

Fig. (6) shows the density distribution for the Shu-Osher problem. This problem includes an interaction between an entropy wave and a shock wave and resolution of density oscillations after the shock is a good criteria for investigate the resolution of a numerical method. The reference solution this problem is calculated by a fifth order WENO-JS [1] scheme. All ACU-WCNS show good numerical resolution and their resolution is superior to that of ninth order WENO-Z.

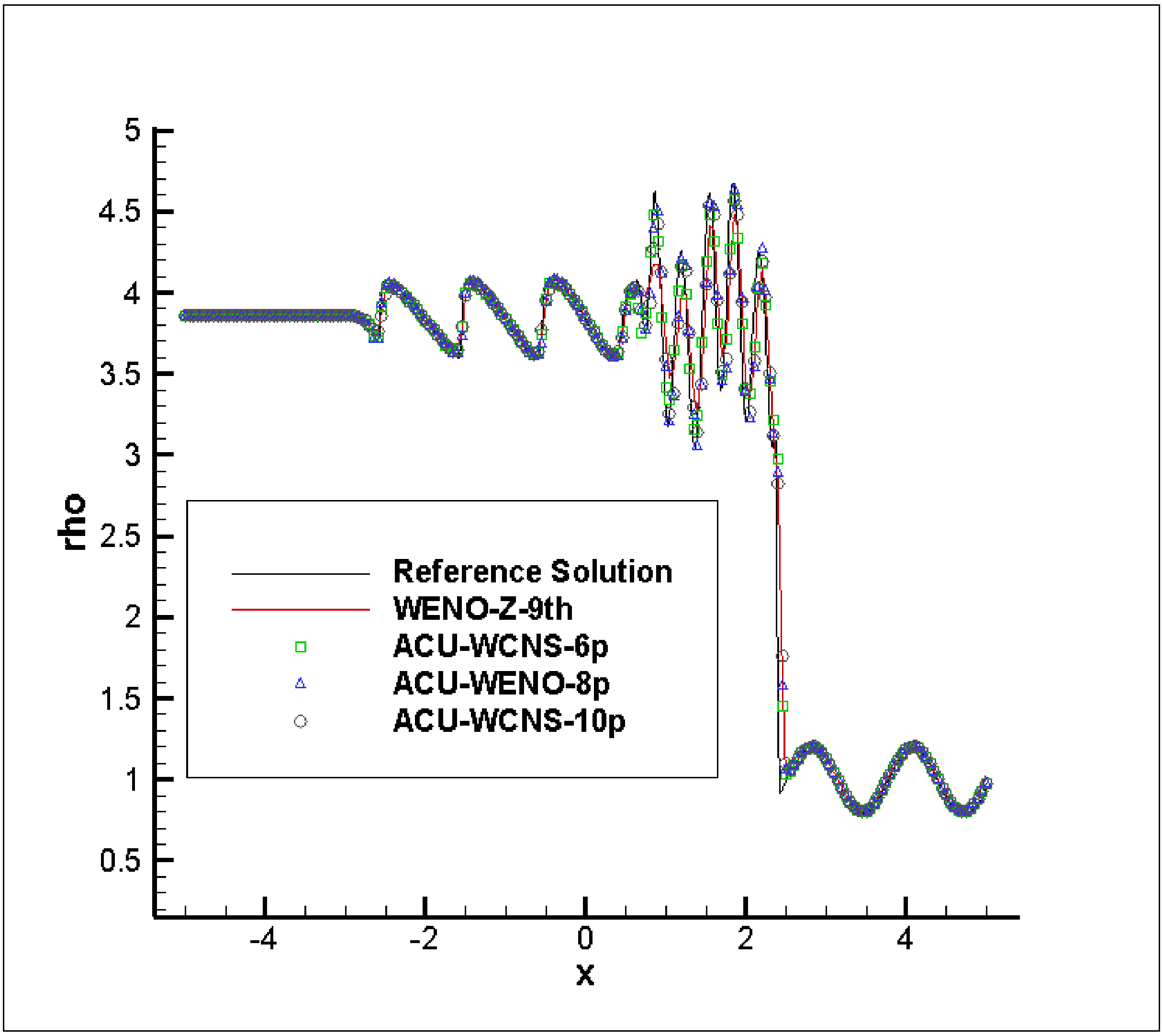

Figure 6. Density distribution for the Shu-Osher problem with 200 grid points t=1.8 s

Conclusions

In this paper we developed an adaptive interpolation procedure for WCNS scheme which adapts between upwind and central stencil based on smoothness of solution. The shock-capturing capabilities of the new scheme and its robustness was tested by solving several benchmark problems. The results of benchmark problems shows the new scheme has good shock capturing capabilities and high numerical resolution.

Appendix A

To avoid exceeding the limit for number of pages in a paper, we omitted the values and formulas for d_k^r, $\hat{f}^{\,r}_{k,i+\frac{1}{2}}$, IS_k^r, IS_{2r} and IS_{ave}^r are given for $r=3$ and $r=4$ and only give these values and formulas for $r=5$.

$$d_0^5=\frac{1}{512},d_1^5=\frac{45}{512},d_2^5=\frac{105}{256},d_3^5=\frac{105}{256},d_4^5=\frac{45}{512},d_5^5=\frac{1}{512}. \qquad \text{(A11)}$$

$$
\begin{cases}
\hat{f}^{5}_{0,i+\frac{1}{2}} = \frac{35}{128} f_{i-4} - \frac{45}{32} f_{i-3} + \frac{189}{64} f_{i-2} - \frac{105}{32} f_{i-1} + \frac{315}{128} f_{i} \\
\hat{f}^{5}_{1,i+\frac{1}{2}} = -\frac{5}{128} f_{i-3} + \frac{7}{32} f_{i-2} - \frac{35}{64} f_{i-1} + \frac{35}{32} f_{i} + \frac{35}{128} f_{i+1} \\
\hat{f}^{5}_{2,i+\frac{1}{2}} = \frac{3}{128} f_{i-2} - \frac{5}{32} f_{i-1} + \frac{45}{64} f_{i} + \frac{15}{32} f_{i+1} - \frac{5}{128} f_{i+2} \\
\hat{f}^{5}_{3,i+\frac{1}{2}} = -\frac{5}{128} f_{i-1} + \frac{15}{32} f_{i} + \frac{45}{64} f_{i+1} - \frac{5}{32} f_{i+2} + \frac{3}{128} f_{i+3} \\
\hat{f}^{5}_{4,i+\frac{1}{2}} = \frac{35}{128} f_{i} + \frac{35}{32} f_{i+1} - \frac{35}{64} f_{i+2} + \frac{7}{32} f_{i+3} - \frac{5}{128} f_{i+4} \\
\hat{f}^{5}_{5,i+\frac{1}{2}} = \frac{35}{128} f_{i+5} - \frac{45}{32} f_{i+4} + \frac{189}{64} f_{i+3} - \frac{105}{32} f_{i+2} + \frac{315}{128} f_{i+1}
\end{cases} . \tag{A12}
$$

$$
\left\{
\begin{aligned}
IS_0^5 &= -\frac{2569471 f_{i-4} f_{i-3}}{60480} + \frac{1501039 f_{-4} f_{i-2}}{20160} - \frac{3568693 f_{i-4} f_{i-1}}{60480} + \frac{1076779 f_{i-4} f_i}{60480} + \frac{5951369 f_{i-3}{}^2}{60480} \\
&\quad - \frac{1751863 f_{i-3} f_{i-2}}{5040} + \frac{8405471 f_{i-3} f_{i-1}}{30240} - \frac{5121853 f_{i-3} f_i}{60480} + \frac{2085371 f_{i-2}{}^2}{6720} - \frac{2536843 f_{i-2} f_{i-1}}{5040} \\
&\quad + \frac{3141559 f_{i-2} f_i}{20160} + \frac{12627689 f_{i-1}{}^2}{60480} - \frac{8055511 f_{i-1} f_i}{60480} + \frac{668977 f_i^2}{30240} + \frac{139567 f_{i-4}{}^2}{30240} \\
IS_1^5 &= \frac{221869 f_{i-3} f_{i+1}}{60480} - \frac{1079563 f_{i-2} f_{i+1}}{60480} + \frac{671329 f_{i-1} f_{i+1}}{20160} - \frac{1714561 f_i f_{i+1}}{60480} + \frac{139567 f_{i+1}{}^2}{30240} \\
&\quad + \frac{20591 f_{i-3}{}^2}{15120} - \frac{725461 f_{i-3} f_{i-2}}{60480} + \frac{395389 f_{i-3} f_{i-1}}{20160} - \frac{847303 f_{i-3} f_i}{60480} + \frac{1650569 f_{i-2}{}^2}{60480} \\
&\quad - \frac{57821 f_{i-2} f_{i-1}}{630} + \frac{2027351 f_{i-2} f_i}{30240} + \frac{539351 f_{i-1}{}^2}{6720} - \frac{306569 f_{i-1} f_i}{2520} + \frac{2932409 f_i^2}{60480} \\
IS_2^5 &= \frac{20591 f_{i+2}{}^2}{15120} + \frac{98179 f_{i-2} f_{i+2}}{60480} - \frac{461113 f_{i-1} f_{i+2}}{60480} + \frac{266659 f_i f_{i+2}}{20160} - \frac{601771 f_{i+1} f_{i+2}}{60480} \\
&\quad - \frac{461113 f_{i-2} f_{i+1}}{60480} + \frac{1050431 f_{i-1} f_{i+1}}{30240} - \frac{291313 f_i f_{i+1}}{5040} + \frac{1228889 f_{i+1}{}^2}{60480} + \frac{20591 f_{i-2}{}^2}{15120} \\
&\quad - \frac{601771 f_{i-2} f_{i-1}}{60480} + \frac{266659 f_{i-2} f_i}{20160} + \frac{1228889 f_{i-1}{}^2}{60480} - \frac{291313 f_{i-1} f_i}{5040} + \frac{299531 f_i^2}{6720} \\
IS_3^5 &= \frac{221869 f_{i-1} f_{i+3}}{60480} - \frac{847303 f_i f_{i+3}}{60480} + \frac{395389 f_{i+1} f_{i+3}}{20160} - \frac{725461 f_{i+2} f_{i+3}}{60480} + \frac{20591 f_{i+3}{}^2}{15120} \\
&\quad + \frac{1650569 f_{i+2}{}^2}{60480} - \frac{1079563 f_{i-1} f_{i+2}}{60480} + \frac{2027351 f_i f_{i+2}}{30240} - \frac{57821 f_{i+1} f_{i+2}}{630} + \frac{671329 f_{i-1} f_{i+1}}{20160} \\
&\quad - \frac{306569 f_i f_{i+1}}{2520} + \frac{539351 f_{i+1}{}^2}{6720} + \frac{139567 f_{i-1}{}^2}{30240} - \frac{1714561 f_{i-1} f_i}{60480} + \frac{2932409 f_i^2}{60480} \\
IS_4^5 &= -\frac{5121853 f_i f_{i+3}}{60480} + \frac{8405471 f_{i+1} f_{i+3}}{30240} - \frac{1751863 f_{i+2} f_{i+3}}{5040} + \frac{5951369 f_{i+3}{}^2}{60480} + \frac{1076779 f_i f_{i+4}}{60480} \\
&\quad - \frac{3568693 f_{i+1} f_{i+4}}{60480} + \frac{1501039 f_{i+2} f_{i+4}}{20160} - \frac{2569471 f_{i+3} f_{i+4}}{60480} + \frac{139567 f_{i+4}{}^2}{30240} + \frac{2085371 f_{i+2}{}^2}{6720} \\
&\quad + \frac{3141559 f_i f_{i+2}}{20160} - \frac{2536843 f_{i+1} f_{i+2}}{5040} - \frac{8055511 f_i f_{i+1}}{60480} + \frac{12627689 f_{i+1}{}^2}{60480} + \frac{668977 f_i^2}{30240} \\
IS_5^5 &= \frac{14813989 f_{i+1} f_{i+3}}{20160} - \frac{2982247 f_{i+2} f_{i+3}}{1260} + \frac{9836471 f_{i+3}{}^2}{6720} - \frac{24804943 f_{i+1} f_{i+4}}{60480} + \frac{40203671 f_{i+2} f_{i+4}}{30240} \\
&\quad - \frac{4166159 f_{i+3} f_{i+4}}{2520} + \frac{28344089 f_{i+4}{}^2}{60480} + \frac{5324029 f_{i+1} f_{i+5}}{60480} - \frac{17334403 f_{i+2} f_{i+5}}{60480} + \frac{7212409 f_{i+3} f_{i+5}}{20160} \\
&\quad - \frac{12302761 f_{i+4} f_{i+5}}{60480} + \frac{668977 f_{i+5}{}^2}{30240} + \frac{58316969 f_{i+2}{}^2}{60480} - \frac{36559021 f_{i+1} f_{i+2}}{60480} + \frac{724873 f_{i+1}{}^2}{7560}
\end{aligned}
\right. \qquad (A13)
$$

$$
\begin{aligned}
IS_{10} = {} & \frac{6256522469005275648 59 f_{i-1} f_{i+3}}{72844785274060800} - \frac{9505458619090627988189 f_i f_{i+3}}{728447852740608000} \\
& + \frac{9507517967943533533133 f_{i+1} f_{i+3}}{728447852740608000} - \frac{3130783545165186871223 f_{i+2} f_{i+3}}{364223926370304000} \\
& + \frac{1309941690301995642707 {f_{i+3}}^2}{728447852740608000} + \frac{8872052170732477009253 f_i f_{i+4}}{2913791410962432000} \\
& - \frac{8969401895441394272981 f_{i+1} f_{i+4}}{2913791410962432000} + \frac{2715884744243791857 41 f_{i+2} f_{i+4}}{132445064134656000} \\
& - \frac{2530080068951963069 59 f_{i+3} f_{i+4}}{291379141096243200} + \frac{12367907231202022338 59 {f_{i+4}}^2}{11655165643849728000} \\
& + \frac{9326436977172514729 57 f_{i+1} f_{i+5}}{2913791410962432000} - \frac{387522890789727688 7 f_{i+2} f_{i+5}}{17986366734336000} \\
& + \frac{103409966285295415 51 f_{i+3} f_{i+5}}{112068900421632000} - \frac{492789997501135891 3 f_{i+4} f_{i+5}}{215836400812032000} \\
& + \frac{395559195760415965 9 {f_{i+5}}^2}{3178681539231744000} - \frac{1034236639532760969 67 f_{i-4} f_{i+1}}{264890128269312000} \\
& + \frac{529970574000000207 91 f_{i-4} f_{i+2}}{22413780084326400} - \frac{1482716738316457541 9 f_{i-4} f_{i+3}}{161877300609024000} \\
& + \frac{1201492985433636796 27 f_{i-4} f_{i+4}}{5827582821924864000} - \frac{3595521736053749053 7 f_{i-4} f_{i+5}}{17482748465774592000} \\
& - \frac{2479311724775857034 51 f_{i-3} f_{i+2}}{112068900421632000} + \frac{969312293783927624 39 f_{i-3} f_{i+3}}{112068900421632000} \\
& - \frac{11438582485973641878 59 f_{i-3} f_{i+4}}{5827582821924864000} + \frac{11494084832115018308 3 f_{i-3} f_{i+5}}{5827582821924864000} \\
& - \frac{266829112930057383 23 f_{i-2} f_{i+3}}{7433141354496000} + \frac{368352134603817782 3 f_{i-2} f_{i+4}}{4482756016865280} \\
& - \frac{1212215737967781346 43 f_{i-2} f_{i+5}}{14568957054812160 00} - \frac{2223776829027201867 47 f_{i-1} f_{i+4}}{112068900421632000} \\
& + \frac{756742571744038456 1 f_{i-1} f_{i+5}}{37356300140544000} - \frac{395559195760415965 9 f_i f_{i+5}}{12613815631872000} \\
& + \frac{983804843910161900 71 {f_{i+2}}^2}{9460361723904000} + \frac{3311611232916529587463 f_{i-2} f_{i+2}}{364223926370304000} \\
& - \frac{1120112685403347800557 f_{i-1} f_{i+2}}{52031989481472000} + \frac{3365674159325425003583 f_i f_{i+2}}{104063978962944000} \\
& - \frac{266147075946973987 79 f_{i+1} f_{i+2}}{832511831703552} + \frac{2106642936305224401793 f_{i-3} f_{i+1}}{582758282192486400} \\
& - \frac{10702066665498073472573 f_{i-2} f_{i+1}}{728447852740608000} + \frac{3577106583060361769087 f_{i-1} f_{i+1}}{104063978962944000} \\
& - \frac{10615118341597060366373 f_i f_{i+1}}{208127957925888000} + \frac{14798321188572635605 79 {f_{i+1}}^2}{59465130835968000} \\
& + \frac{712048756425280794 7 {f_{i-4}}^2}{3178681539231744000} - \frac{444340302953253781 43 f_{i-4} f_{i-3}}{116551656438497280 0}
\end{aligned}
\qquad \text{(A14)}
$$

$$
\begin{aligned}
&+\frac{5335640432737222309 f_{i-4} f_{i-2}}{37356300140544000}-\frac{4506987629438845856103 f_{i-4} f_{i-1}}{1456895705481216000} \\
&+\frac{12447538778094427995 17 f_{i-4} f_i}{2913791410962432000}+\frac{1933473108524561292707 f_{i-3}{}^2}{11655165643849728000} \\
&-\frac{1846150261009678724267 f_{i-3} f_{i-2}}{1456895705481216000}+\frac{369540661282663048781 f_{i-3} f_{i-1}}{132445064134656000} \\
&-\frac{1138600296553219536590 9 f_{i-3} f_i}{2913791410962432000}+\frac{1795138265821207839347 f_{i-2}{}^2}{728447852740608000} \\
&-\frac{803682346250438388043 f_{i-2} f_{i-1}}{72844785274060800}+\frac{163162644963931336474 7 f_{i-2} f_i}{104063978962944000} \\
&+\frac{118705851264711881047 f_{i-1}{}^2}{9460361723904000}-\frac{3766828957892473535791 f_{i-1} f_i}{104063978962944000} \\
&+\frac{1102594454913534130066 1 f_i^2}{416255915851776000}.
\end{aligned}
$$

$$
IS_{ave}^5=\frac{1}{16}\left(3IS_1^5+10IS_2^5+3IS_3^5\right). \tag{A15}
$$

References

[1] Jiang, G. S. and Shu, C. W. (1996) Efficient Implementation of Weighted ENO Schemes, *Journal of Computational Physics* **126(1)**, 202-228.
[2] Deng, X. and Zhang, H. (2000) Developing High-Order Weighted Compact Nonlinear Schemes, *Journal of Computational Physics* **165(1)**, 22-44.
[3] Harten, A., Engquist, B., Osher, S. and Chakravarthy, S. R. (1987) Uniformly high order accurate essentially non-oscillatory schemes, III, *Journal of Computational Physics* **71(2)**, 231-303.
[4] Liu, X. D., Osher, S. and Chan, T. (1994) Weighted essentially non-oscillatory schemes, *Journal of Computational Physics* **115(1)**, 200-212.
[5] Balsara, D. S. and Shu, C. W. (2000) Monotonicity Preserving Weighted Essentially Non-oscillatory Schemes with Increasingly High Order of Accuracy, *Journal of Computational Physics* **160(2)**, 405-452.
[6] Gerolymos, G. A., Senechal, D. and Vallet, I. (2009) Very-high-order WENO schemes, *Journal of Computational Physics* **228(23)**, 8481–8524.
[7] Henrick, A. K., Aslam, T. D. and Powers, J. M. (2005) Mapped weighted essentially non-oscillatory schemes-Achieving optimal order near critical points, *Journal of Computational Physics* **207(2)**, 542-567.
[8] Borges, R., Carmona, M., Costa, B. and Don, W. S. (2008) An improved weighted essentially non-oscillatory scheme for hyperbolic conservation laws, *Journal of Computational Physics* **227(6)**, 3191-3211.
[9] Castro, M., Costa, B. and Don, W. S. (2011) High order weighted essentially non-oscillatory WENO-Z schemes for hyperbolic conservation laws, *Journal of Computational Physics* **230(5)**, 1766-1792.
[10] Pirozzoli, S. (2002) Conservative hybrid compact-WENO schemes for shock-turbulence interaction, *Journal of Computational Physics* **178(1)**, 81-117.
[11] Ren, X. Y., Liu, M, and Zhang, H. (2003) A characteristic-wise hybrid compact-WENO scheme for solving hyperbolic conservation laws, *Journal of Computational Physics* **192(2)**, 365-386.
[12] Kim, D. and Kwon, J. H. (2005) A high-order accurate hybrid scheme using a central flux scheme and a WENO scheme for compressible flow field analysis, *Journal* of *Computational Physics* **210(2)**, 554-583.
[13] Weirs, V. G. and Candler, G. V. (1997) Optimization of Weighted ENO Schemes for DNS of Compressible Turbulence, *AIAA Paper 97–1940*.
[14] Wang, Z. J. and Chen, R. F. (2001) Optimized weighted essentially nonoscillatory schemes for linear waves with discontinuity, *Journal of Computational Physics* **174(1)**, 381-404.
[15] Martín, M.P., Taylor, E.M., Wu, M. and Weirs, V.G. (2006) A bandwidth-optimized WENO scheme for the effective direct numerical simulation of compressible turbulence, *Journal of Computational Physics,* **220(1)**, 270-289.
[16] Tam, C. K. and Webb, J. C. (1993) Dispersion-relation-preserving finite difference schemes for computational acoustics, *Journal of computational physics,* **107(2)**, 262-281.

[17] Zhuang, M. and Chen, R. F. (1998) Optimized upwind dispersion-relation-preserving finite difference scheme for computational aeroacoustics. *AIAA journal*, **36(11)**, 2146-2148.
[18] Yamaleev, N. K. and Carpenter, M. H. (2009) A systematic methodology for constructing high-order energy stable WENO schemes. *Journal of Computational Physics*, ***228*(11)**, 4248-4272.
[19] Hu, X. Y., Wang, Q. and Adams, N. A. (2010) An adaptive central-upwind weighted essentially non-oscillatory scheme, *Journal of Computational Physics* **229(23)**, 8952-8965.
[20] Hu, X. Y. and Adams, N. A. (2011) Scale separation for implicit large eddy simulation. *Journal of Computational Physics*, **230(19)**, 7240-7249.
[21] Deng, X. and Zhang, H. (2000) Developing high-order weighted compact nonlinear schemes. *Journal of Computational Physics*, **165(1)**, 22-44.
[22] Nonomura, T., Iizuka, N. and Fujii, K. (2007) Increasing order of accuracy of weighted compact nonlinear scheme, *AIAA paper 2007-893*.
[23] Zhang, S., Jiang, S. and Shu, C. W. (2008) Development of nonlinear weighted compact schemes with increasingly higher order accuracy *Journal of Computational Physics*, **227(15)**, 7294-7321.
[24] Lele, S.K. (1992) Compact finite difference schemes with spectral-like resolution, *Journal of computational physics*, **103(1)**, 16-42.
[25] Shu, C.W. (2009) High order weighted essentially nonoscillatory schemes for convection dominated problems, *SIAM review*, **51(1)**, 82-126.
[26] Nonomura, T. and Fujii, K. (2013) Robust explicit formulation of weighted compact nonlinear scheme, *Computer & Fluids* **85**, 8-18.
[27] Nonomura, T., Iizuka, N. and Fujii, K. (2010) Freestream and vortex preservation properties of high-order WENO and WCNS on curvilinear grids, *Computers & Fluids*, ***39*(2)**, 197-214.
[28] Nonomura, T. and Fujii, K. (2009) Effects of difference scheme type in high-order weighted compact nonlinear schemes, *Journal of Computational Physics*, ***228*(10)**, 3533-3539.
[29] Sumi, T. and Kurotaki, T. (2015) A new central compact finite difference formula for improving robustness in weighted compact nonlinear schemes, *Computers & Fluids*, **123**, 162-182.
[30] Shi, J., Zhang, Y.T. and Shu, C.W. (2003) Resolution of high order WENO schemes for complicated flow structures, *Journal of Computational Physics*, **186(2)**, 690-696.
[31] Zhang, Y.T., Shi, J., Shu, C.W. and Zhou, Y. (2003) Numerical viscosity and resolution of high-order weighted essentially nonoscillatory schemes for compressible flows with high Reynolds numbers, *Physical Review E*, **68(4)**, 046709.
[32] Berland, J., Bogey, C. and Bailly, C. (2008) A study of differentiation errors in large-eddy simulations based on the EDQNM theory, *Journal of Computational Physics*, **227(18)**, 8314-8340.
[33] Shu, C.W. and Osher, S. (1988) Efficient implementation of essentially non-oscillatory shock-capturing schemes. *Journal of Computational Physics*, **77(2)**, 439-471.
[34] Sod, G.A. (1978) A survey of several finite difference methods for systems of nonlinear hyperbolic conservation laws, *Journal of computational physics*, **27(1)**, 1-31.
[35] Lax, P.D. (1954) Weak solutions of nonlinear hyperbolic equations and their numerical computation, *Communications on pure and applied mathematics*, **7(1)**, 159-193.
[36] Einfeldt, B., Munz, C.D., Roe, P.L. and Sjögreen, B. (1991) On Godunov-type methods near low densities, *Journal of computational physics*, **92(2)**, 273-295.
[37] Toro, E. F. (2009) *Riemann solvers and numerical methods for fluid dynamics: a practical introduction*, 3rd edn, Springer, Berlin, Germany.
[38] Shu, C.W. and Osher, S. (1989) Efficient implementation of essentially non-oscillatory shock-capturing schemes, II, *Journal of Computational Physics*, **83(1)**, 32-78.